Synthesis and Antibacterial Investigation of ZnO/CNPs Nanocomposite Powder by Hot Nickel Plate Assisted Cost Effective Spray Pyrolysis Method and its Characterizations

D. Saravanakkumar[1], S. Sivaranjani[2], S. Karthi[3], S.Pandiarajan[4], B.Ravikumar[5]

[1]*Research Scholar, Research and Development Centre,Bharathiar University, Coimbatore, Tamilnadu, India*
[2]*Research guide, R&D centre, Bharathiar University, Coimbatore, India and Assistant Professor, Department of Physics, SBM College of Engineering and Technology, Dindigul- 624 005, Tamilnadu, India*
[3, 4, 5] *Department of Physics, Devanga Arts College (Autonomous), Aruppukottai, 626101, Tamilnadu, India*
Corresponding author Email: dskapk@gmail.com

Abstract: *Nanocomposite powder containing Zinc oxide and carbon nano particles (ZnO/CNPs) has been synthesized by a cost effective hot nickel plate assisted simplified spray pyrolysis method using zinc acetate dihydrate as host precursor source and sugar as carbon source. The structure, optical properties and morphologies of ZnOnanoflakes have been characterized by X-ray diffraction (XRD), UV–Vis spectrophotometry, Fourier transform infrared (FTIR), scanning electron microscopy (SEM) and energy dispersive X-ray analysis (EDAX).The antibacterial study against both gram positive and negative bacteria has been studied by well diffusion method. The SEM analysisreveals the formation of ZnOnanoflakes. XRD shows the hexagonal structure of the ZnOnanoflakes. Strong blue shift absorption is observed from the UV–vis spectrophotometry.*

Keywords:*Antibacterial study, Nano composite, Optical properties, Spray Pyrolysis, Structural Properties.*

I. Introduction

In current trends, countlessconcentration has been stimulated in the antibacterial studies for different bacteria using ZnONPs of organic contamination by various experimental method. Zinc oxide (ZnO) is an n-type semiconductor with a wide direct band gap of 3.37 eV, which is a promising photocatalyst used extensively for the photocatalytic degradation of different water pollutants because of its low cost, high activity, and environment friendly features. ZnO has perhaps the richest family of nanostructures among all materials, both in structures and properties. A variety of ZnO nanostructures, such as nanowires, nanotubes, nanofibers, nanospheres and nano-tetrapods, nano-cabbage, nanocombs, nanowalls and nanoprisms have been successfully grown by different methods including vapour-liquid-solid (VLS) technique, thermal evaporation, low temperature aqueous chemical growth (ACG), electrodeposition, etcNano-scale particles of ZnO possess a high surface area to volume ratio [1-4]. It possesses many importantapplications in electronic and optical devices. Though ZnO is one of the vastly deliberated materials for solarcells, gas sensors, optoelectronic applications, etc., owing to its excellent optical and electrical properties. A common low cost method to produce ZnO NPs are to first produce chemically modified by using chemical routes and temperature annealing. ZnO NPs have potential application in optoelectronic devices, such as in organic light emitting diodes and organic solar cells as atransparent electrode material. The ZnO thin film crystal and its structural properties strongly depend on growth technique and growth condition. Many fabrication methodologies and top–down approaches have been applied to obtain high quality nano/micro structured ZnO NPs [5,6].

The emergence of carbon nanoparticle (CNPs) shows high potential in biological labeling, bioimaging and other different optoelectronic device applications. Carbon nano particles/tubes/fibers are the most researched materials of the 21st century with an international intention of growing industrial quantities due to their unique properties such as good electrical/thermal conductivity, enhanced chemical/bio compatibility and excellent corrosion resistance for wide range of applications which include polymer composites, electrochemical energy storage and conversion, filtration, hydrogen storage, catalysis and biotechnology. Successful utilization of carbon nanoparticles in various applications is strongly dependent on the development of simple, efficient and inexpensive technology for its production [7-10].Common routes in making carbon nanoparticle includes high energy ion beam radiation based creation of point defect in diamond particle followed by annealing laser ablation of graphite followed by oxidation and functionalizationthermal decomposition of organic compound, electrooxidation of graphite and oxidation of candle soot with nitric acid[11-14].

The various synthesis routes have been reported for the preparation of ZnO nanoparticle. The notable examples are simplifies spray pyrolysis method, copreparation method, sol-gel , solvothermal , microemulsion physical methods including chemical vapor deposition, gel cumbution method, thermal decomposition of

organometallic precursors, arc plasma, laser ablation, and levitation gas condensation reverse micelles process, salt reduction, microwave dielectric heating reduction, ultrasonic irradiation, radiolysis, electrochemical synthesis etc.,[15-21]

The presents work describes the synthesis of carbon nano particles doped ZnOnano particles using simplified spray pyrolysis method with some modified experimental arrangement. Number of research work has been reported using this method for preparing thin films only. In the present work, the title compound is prepared in an slightly different from spray pyrolysis method which is cost effective and simple.

II.   Materials And Methods

Zinc acetate dihydrate (Sigma Aldrich, 99% purity) was taken as precursor. Zinc acetate of 0.05 M precursor solution made of 50 ml of deionized water was used to synthesis ZnO nanoparticles. In the first step, sugar (stevia sugar purity 99%) solution of 0.01 M is mixed with precursor solution. Then it is stirred for 2 hours at 50˚C. In this case sugar mainly acts as carbon source. In second step the mixed solution is poured into the perfume spray atomizer without any other impurity. In third step, the nickel plate in the dimension of 15cmx12cmx1mm is placed on the hot plate at 200˚C. In fourth step the mixed solution is sprayed nearly 100 times directly on the hot nickel plate with 5 seconds interval and then it is cooled for 30 minutes. Then, deposited ZnO/CNPs nano composite powder removed by fine metal strip and collected in glass tube named as sample A. The same procedure is followed for sample B having 0.02 Msugar solution where concentration of precursor solution is constant.

After final preparation, the particles were dried at 80 °C and normal pressure and ground to a fine powder with a pestle and mortar. Finally it is calcined at 150˚ for 8 hours in muffle furnace.

The structural characterization of both the ZnO/CNPs nano powder were carried out using X-ray diffraction technique employing with Cu source. Absorption spectra were recorded on UV-Visible spectrophotometer study (Shimadzu-1700 series) and the Fourier Transform Infrared (FTIR spectra Shimadzu IR) studies were done for as prepared samples.

III.   Result and Discussion

3.1 XRD Analysis

The X-ray diffraction (XRD) pattern of ZnO/CNPs nano particles powder is shown in Fig.3.1where peaks at 2θ values are 24.0852, 31.7695, 34.4445, 36.2533, 47.5875, 56.6214, 62.9526, 67.9950 ,69.2302 for sample A and 23.8050, 31.7622, 34.3898, 36.2361, 47.5547, 56.5902, 62.8360, 67.9780, 69.0242 Fig.3.1for sample B can be associated with (100), (002), (101), (102), (110), (103), (200), (112) and (201) planes respectively. The ZnO product shows hexagonal structure with primitive lattice, which are in good agreement with other literatures [22].The patterns are in accord with the typical zincite structure ZnO diffraction where hexagonal phase, spacegroup $P6_3mc$, with lattice constants $a = 3.24982$ Å, $c = 1.6021$ Å, $Z = 2$, JCPDS No. 36-1451etc.The average particle size (D) was determined using the Scherer s equation $D = 0.9\lambda / \beta\cos\Theta$, where D is the crystallite size, K is the shape factor, being equal to 0.9 , λ is the X-ray wavelength, β is the full width at half maximum of the diffraction peak, and Ө is the Bragg diffraction angle in degree. The average particles size was found to be in the range of 24-31nm [23]. The sharpness of peaks shows that ZnO NPs are highly crystalline nature.
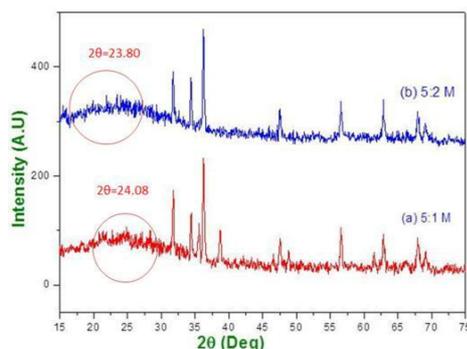

Fig 3.1 XRD Spectrum OfZno/CnpsNanocomposites For Sample A (Red) And Sample B (Blue)

The analysis of carbon nano particles with ZnONPs was carried out to identify their crystal structure. The XRD spectrum shows that there are two Bragg diffraction broad peaks at near $2\theta = 23.68^\circ$ It has been reported that the XRD peak at near $2\theta = 23.68^\circ$ indexed as (002) is an indication of the presence of large amounts of amorphous material in association with multi-walled carbon nano tubes [24, 25]. In the present study, the peaks at near $2\theta = 23.80^\circ$ and 24.08˚ were indexed as (002) plane which correspond to the presence of

less amounts of amorphous MWCNT CNPs in association with hexagonal graphite lattice. The crystal structure parameter such as crystallite size D, d - spacing, crystallites volume V, lattice parameter a & c, *c/a* ratio, cell volume v,number of unit cells NU, bond length ιand dislocation density δ of ZnO/CNPs nanocompsite calculated from XRD data are tabulated in the Table.1

Sample	2Θ	D Nm	d (Å)	V (nm)^3	Lattice Constant			v (Å)^3	NU x10^6	ι (Å)	δX 10^{-4} nm^{-2}
					a (Å)	c (Å)	c/a				
A	36.271	24.49	2.474	67.34	3.244	5.206	1.604	57.012	3.594	1.873	5.537
B	36.236	31.37	2.815	70.25	3.243	5.217	1.608	54.076	3.701	1.836	6.788

Table.1 Crystallite size, d - spacing, Crystallites volume, Lattice parameter, c/a ratio, cell volume, Number of unit cell, Bond length and dislocation density of ZnO/CNPs nanocompsite calculated from XRD data.

3.2 SEM Analysis

SEMmicrograph of ZnO/CNPs composite obtained from simplified spray pyrolysis withhot nickel plate assistance method. The SEM analysis was used to determine the structure of the reaction products that were formed. SEM image has showed carbon nanoparicles covered zinc oxide nano particles with more number of aggregates as well. The SEM image showed relatively flake like nanoparticles shown in high magnification SEM structure, with appearance some agglomerated grain groups. Figure 3.2 (a) shows SEM image of the NPs from the solution of 5:1 volumetric ratio of Zinc acetate/sugar mixture S-A. Increasing the Zinc acetate/sugar ratio to 5:2S-B, the agglomeration seems more pronounced and agglomerated groups are layered. However it is clearly seen that the presence of MWCNTs yield a large number of ZnO nanoparticles mostly with irregular shape and size Fig. 3.2 (b). Some particles display an appearance of hexagonal nanoplates, indicating uniform growth of ZnO nanostructures.
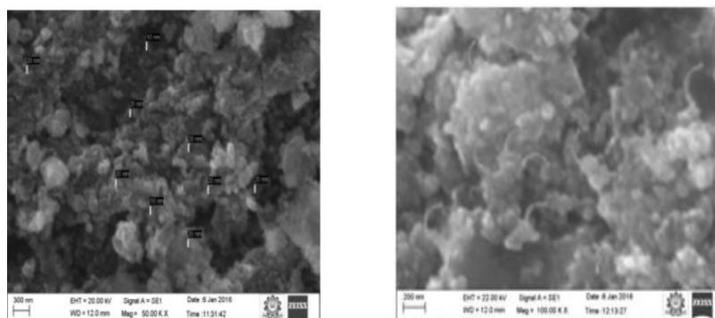

Fig. 3.2 (a) SEM micrgraph of   Fig. 3.2 (b) SEM micrgraph of
ZnO/CNPs for S-A   ZnO/CNPs for S-B

The EDAX pattern in the fig 3.2 (c) reveals that only signals from O, Zn and C can be detected. In addition, no trace of other element such as k, S, P, Cr detected in the EDX pattern, indicating that the nanowires are pure ZnO/CNPs nano composite.
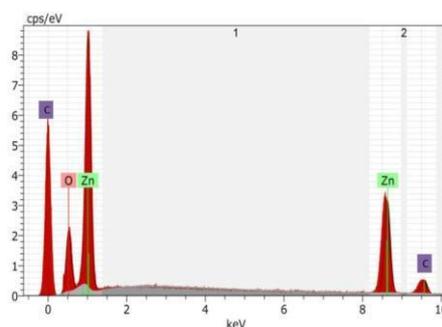

Fig 3.2 (c) EDAX spectrum of of ZnO/CNPs for S-B

3.3 FTIR Analysis

Infrared (IR) spectroscopy is a popular characterization technique in which a sample is placed in the path of an IR radiation source and its absorption of different IR frequencies is measured. Solid, liquid, and gaseous samples can all be characterized by this technique. The FTIR spectrum of ZnO/CNPs nanostructure was recorded in the range 400-4000 cm^{-1}, using FTIR spectrometer and is given in Figure 3.3 (a). The band between the 450-500 cm^{-1} corelated to metal oxide bond (ZnO).
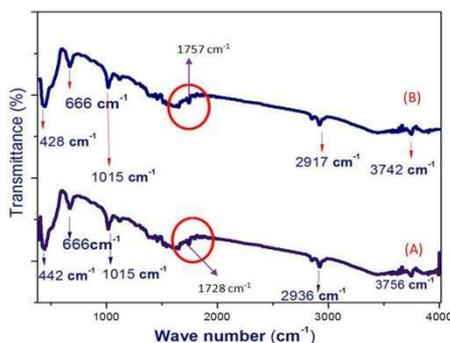

Fig 3.3 (a) FTIR spectrum of ZnO/CNPs Nanocomposites for sample A and B

The structural analysis of wurtziteZnO was further supported through FTIR investigation corresponds to the wurtzite oxide stretching frequencies of ZnO. The main absorption bands at ~ 450–500 cm^{-1} are due to the stretching mode of ZnO. From the FTIR spectrum, various functional groups and metal-oxide (MO) bond present in the compound were analyzed, where absorption peak at 428 cm^{-1}, 442 cm^{-1} and 666 cm^{-1} are attributed to stretching vibrations of Zn-O bonds. It confirms the presence of ZnOnano particles. Also the sharp bands at 1015 cm^{-1} and 1016 cm^{-1} indicate the symmetric stretching of C-O group present in the extract [26]. The absorption band at 2920 cm-1 can be ascribed to the stretching mode of C-H bonds and its shift to 2936 cm^{-1} and 2917 cm^{-1} in synthesized ZnO NPs. The peaks at 3742 cm^{-1} and 3756 cm^{-1} indicate the presence of O-H residue probably due to atmospheric moisture [27]. FTIR spectroscopy given further evidence of MWCNT-O–C=O group that existed on the surface, and its characteristic weak absorption peak of 1728cm^{-1} and 1756 cm^{-1} were observed for the samples A and B.Formation of ZnO/CNPs nanocomposite prepared by this method such particles on the surface of disordered multi-walled CNTs (ZnO/MWCNTs) is possible from the sugar molecular carbon source [28]. The SEM and EDAX results confirm the presence of noble CNPs and ZnO nanoparticles

3.4 UV-Vis Spectra Analysis

The electronic absorption spectrum of ZnO samples in the UV-vis range enables to characterize the absorption edge related to semiconductor band structure. The direct band gap energy (E_g) for the ZnOnanocrystals is determined by fitting the reflection data tothe direct transition equation $\alpha h v = A (h v - E_g)^n$, where$\alpha$is the optical absorption coefficient, $hv$is the photon energy, $E_g$is the direct band gap and A is a constant and 'n' depends on the kind of optical transition that prevails. Specifically, with $n = 1/2$, a good linearity has been observed for the direct allowed transition, the most preferable one in the system studied here by replacing $n = 1/m$ which are n = 2 for allowed direct transition, n = ½ for allowed indirect, n = 1/3 for forbidden indirect and n = 2/3 for forbidden direct of optical transitions The exact value of the band gap is determined by extrapolating the straight line portion of $(\alpha h v)^2$ Vs$hv$to the x axis.Fig.3.4 (a)shows the absorption spectrumof the ZnO/CNPs composite with a sharp absorptionpeak at 349.393 nmwhich corresponds to a blue-shift of 15±2 nm compared to bulk ZnO [29, 30].
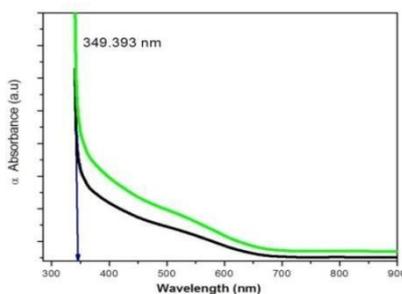

Fig 3.4 (a) UV-Vis Absorption spectrum of the ZnO/CNPs nanocomposite Sample A (black) & B (green)

Fig.3.4 (b) shows the variation of $(\alpha h v)^{1/n}$ vs. photon energy, hvfor as synthesized ZnO/CNPs nano particles with n values of 1/2. Allowed direct band gap of ZnOnano particles is calculated to be 3.3265 eV for S-A and3.3905eV for S-B, which are closer to the reported value 3.37 eV [31].
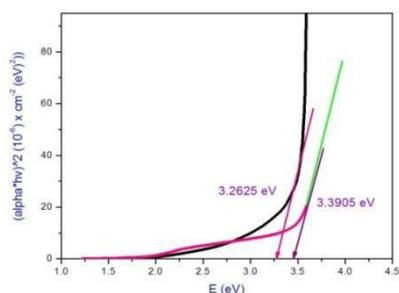

Fig. 3.4 (b) Shows the variation of $(\alpha h v)^{1/n}$Vs photon energy, Sample A (black) & B (pink)

3.5 Antibacterial activity of ZnO/ CNPs (Sample B) against bacterial pathogens using welldiffusion method

Antimicrobial activities of the synthesized Ag doped Bismuth oxide nanoparticles were performed against both Gram-positive [Staphylococcus aureus] and Gram-negative [Pseudomonas aeruginosa] bacteria. Staphylococcus aureus is a gram-positive cocal bacterium that is a member of the Firmicutes, and is frequently found in the nose,respiratory tract, and on the skin. It is often positive for catalase and nitrate reduction. Although S. aureus is not always pathogenic, it is a common cause of skin infections such as abscesses, respiratory infections such as sinusitis, and food poisoning. Pathogenic strains often promote infections by producing potent protein toxins, and expressing cell-surface proteins that bind and inactivate antibodies.Antibacterial activities of the ethanolic extract of the compounds Sample B were determined using well diffusion method. It is performed by sterilizing Mueller Hinton agar media. After solidification, wells were cut on the Mueller Hinton agar using cork borer. The test bacterial pathogens such as Staphylococcus aureus and Pseudomonas aeruginosa were swabbed onto the surface of Mueller Hinton agar plates. Wells were impregnated with 25 µl of the test samples (ethanolic extract of the compounds). The plates were incubated for 30 min to allow the extract to diffuse into the medium. The plates were then incubated at 37°C for 24 hours, and then the diameters of the zone of inhibition were measured in millimetres.

Fig.3.5 (c) Antimicrobial activity of ZnO/ CNPs (Sample B)against *Staphylococcus aureus*

Fig.3.5 (d) Antimicrobial activity of ZnO/ CNPs (Sample B)against *Pseudomonas aeruginosa*

Each antibacterial assay was performed in triplicate and mean values were reported and the photographs showing the inhibition zones around the disks are shown in Fig. 3.5 (c) and (d). The histogram chart representing the zone of inhibition are shown in Fig. 3.5 (e). Antibacterial activity of metal compounds against bacterial pathogens was tabulated in Table.2. From these results, it is found that ZnO/CNPs composite powder exhibits antibacterial nature and its efficiency is higher for gram positive bacteria [Staphylococcus aureus] than Gram-negative [Pseudomonas aeruginosa] bacteria.

Test bacterial pathogens	Zone of inhibition in millimeter (in diameter)
	ZnO/ CNPs (Sample B)
Staphylococcus aureus	33
Pseudomonas aeruginosa	21

Table. 2. Antibacterial activity of metal compounds against bacterial pathogens

Solvent used: Ethanol, ***Standard used***: *Ampicillin 10 µg*
Staphylococcus aureus
Zone of inhibition for Amp 10 µg - 17 mm
Pseudomonas aeruginosa
Zone of inhibition for Amp 10 µg - 12 mm

Fig. 3.5 (e) Antibacterial activity of ZnO/CNPs composite(S-B) against bacterial pathogens

IV.   Conclusion

In the present work, we first report an eco-friendly and simple method for the synthesis of ZnO/CNPs composite using sugar solution.The formation of ZnO/CNPs nanocomposite confirmed by XRD, SEM and EDAX methods. XRD analysis reveals that the average grain size of the nanoparticles was found to be 24-31 nm which was calculated by Debye-Scherrer equation. The formation of ZnO/CNPs nanocomposite was also confirmed by Fourier transform infrared spectroscopy (FTIR). From the FTIR spectrum, the stretching and bending frequencies of the molecular functional groups in the sample were studied. The optical bandgap of as prepared Nano composite were obtained from optical absorption spectra by UV-Vis absorption spectroscopy. Upon increasing the concentration of the sugar solution the optical band gap decreases from 3.39 eV to 3.29 eV. From the antibacterial study the inhibition zone is larger for gram positive bacteria than gram negative bacteria.The method of the present study offers several important advantageous features. The synthesis route is economical and environment friendly, because it involves inexpensive and non-toxic materials for second, large scale synthesis.

Reference

[1]. S. J. Pearson, D. P. N. Orton, K. I., Y. W. Hoe, T. Steiner, Prog. Mat. Sci., 50, 2005, , 293.O. Dulub, L. A. Boatner, U. Diebold, Surf. Sci., 519, 2002, 201.
[2]. Fan Xi-Mei, Zhou Zuo-Wan, Wang Jie and TianKe, Trans. Nanoferrous Met. Soc.China., 21, 2011, 2056.
[3]. Mansidhingra, Lalit Kumar, SadhnaShrivastava, P. Senthil Kumar and S. Annapoorni, Bull.Mater. Sci., 36, 2013, 647 .
[4]. E. H. Kisi, M. M. Elcombe, ActaCryst., 45,1989, 1867.
[5]. J. E. Jaffe, A. C. Hess, Phys. Rev., 48, 1993, 7903.
[6]. L. Gerward and J. S. Olsen, J. Synchrotron Radiat., 2, 1995, 233.
[7]. T. Kogure and Y. Bando, J. Electron Microsc., 1993, 47, 7903.
[8]. A. B. M. A. Ashrafi, A. Ueta, A. Avramescu, H. Kumano, I. Suemune, Y. W. Ok and T.Y.Seong, Appl. Phys. Lett., 76, 2000, 550.
[9]. S. K. Kim, S. Y. Seong and C. R. Cho, Appl. Phys. Lett., 82, 2003, 562.
[10]. C. H. Bates,W. B. White and R. Roy, Science., 137, 1962, 993.
[11]. J. E. Jaffe, J. A. Snyder, Z. Lin and A. C. Hess, Phys. Rev. B., 62, 2000, 1660.
[12]. A. F. Kohan, G. Ceder, D. Morgan and C.G. Van de Walle, Phys. Rev., 61, 2000, B, 15019.
[13]. C.G. Van de Walle, Phys. Rev. Lett., 85, 2000, 1012.
[14]. Asano, H.; Muraki, S.; Endo, H.; Bandow, S.; Iijima, S. J. Phys. Condens. Matt., 22, 2010, 1–6.
[15]. Yang, X.G.; Li, C.; Wang, W.; Yang, B.J.; Zhang, S.Y.; Qian, Y.T, Chem. Commun., 3, 2004, 342–343.
[16]. Lou, Z.S.; Chen, Q.W.; Zhang, Y.F.; Wang, W.; Qian, Y.T, J. Am. Chem. Soc., 125, 2003, 9302–9303.
[17]. Lou, Z.S.; Chen, Q.W.; Zhang, Y.F.; Qian, Y.T.; Wang, W, J. Phys. Chem. B., 108, 2004, 4239–4241.

[18].   D. N. Shooto, and E. D. Dikio, "Morphological Characterization of soot from the combustion ofcandle wax" Int. J. Electrochem. Sci., 6, 2011, 1269-1276.
[19].   E. D. Dikio, "Morphological characterization of soot from the atmospheric combustion of dieselfuel", Int. J. Electrochem., Sci., 6, 2011, 2214-2222.
[20].   Mohammad AbulHossain*, Shahidul Islam, American Journal of Nanoscience and Nanotechnology., 1, 2013, 52-56.
[21].   JayaprakashKhanderi, Rudolf C. Hoffmann and Jeorg J. SchneiderNanoscale., 2, 2010, 613–622,
[22].   613
[23].   E. Mansfield, A. Kar, and S. A. Hooker, "Analytical and Bioanalytical Chemistry., 396, 2010, 1071–1077,.
[24].   L. Wu and Y. Wu, J. Mater. Sci., 42, 2007, 406–408;
[25].   H. Yu, Z. Zhang,M. Han and F. Zhu, J. Am. Chem. Soc., 127, 2005, 2378–2379.
[26].   T. Xia, M. Kovochich, M. Liong, L. Maddler, B. Gilbert, H. Shi, J.I. Yeh, J.I. Zink, A.E.Nel, ACS Nan., 5, 2008, 2121–2134.
[27].   P. Rajiv, S. Rajeshwari , R. Venckatesh, SpectrochimicaActa Part A., 112, 2013, 384–387.
[28].   K. Elumalai , S. Velmurugan , S. Ravi , V. Kathiravan , S. Ashokkumar, SpectrochimicaActa Part A: Molecular and Biomolecular Spectroscopy., 136, 2015, 1052–1057.
[29].   Nanda Shakti, P.S.Gupta, Applied Physics Research, 2, 2010, 19-28.
[30].   S. Rajesh, T. Ganesh, Francis P. Xavier, Journal of Electron Devices, 17, 2013, 1417-1422.
[31].   31 Y. Li, W. Zhang, J. Niu, Y. Chen, ACS Nan., 6, 2012, 5164–5173.